Deterministically entangling multiple remote quantum memories inside an optical cavity

Zhihui Yan,[1,2,*] Yanhong Liu,[1] Jieli Yan,[1] and Xiaojun Jia[1,2]

[1]*State Key Laboratory of Quantum Optics and Quantum Optics Devices, Institute of Opto-Electronics, Shanxi University, Taiyuan 030006, People's Republic of China*

[2]*Collaborative Innovation Center of Extreme Optics, Shanxi University, Taiyuan 030006, People's Republic of China*

(Received 11 August 2017; revised manuscript received 28 December 2017; published 31 January 2018)

Quantum memory for the nonclassical state of light and entanglement among multiple remote quantum nodes hold promise for a large-scale quantum network, however, continuous-variable (CV) memory efficiency and entangled degree are limited due to imperfect implementation. Here we propose a scheme to deterministically entangle multiple distant atomic ensembles based on CV cavity-enhanced quantum memory. The memory efficiency can be improved with the help of cavity-enhanced electromagnetically induced transparency dynamics. A high degree of entanglement among multiple atomic ensembles can be obtained by mapping the quantum state from multiple entangled optical modes into a collection of atomic spin waves inside optical cavities. Besides being of interest in terms of unconditional entanglement among multiple macroscopic objects, our scheme paves the way towards the practical application of quantum networks.

DOI: 10.1103/PhysRevA.97.013856

I. INTRODUCTION

Quantum entanglement is the building block of quantum information [1,2]. With the development of quantum information, quantum networks consisting of quantum channels and quantum nodes have attracted extensive attention [3]. Quantum nodes can be used to store and process quantum information. Atomic ensembles [4–10], single atoms [11,12], trapped ions [13–15], optomechanics [16–19], superconductors [20], solid-state systems [21–24], and other physical systems have been utilized as quantum nodes. The atomic ensemble in particular is an ideal example of a quantum node, with the key advantage of the collective enhancement of the light-atom interaction [4–10]. The quantum network will rely on the ability to generate, store, and distribute entanglement across quantum nodes and thus the generation of entanglement among atomic ensembles is a longstanding goal for the development of quantum networks. Although significant progress has been made in the construction of entanglement between two atomic ensembles by many groups [25–32], producing entanglement among more than two atomic ensembles is harder, which is crucially important for quantum information transmission across the quantum network [33,34] and one-way quantum computation [35]. Recently, discrete-variable (DV) entanglement stored in four atomic ensembles, which is the heralded W state of atomic spin waves, has been obtained by means of the Raman scattering mechanism [36]. In the continuous-variable (CV) regime, which offers another path towards the realization of quantum information, unconditional entanglement among three atomic ensembles has been demonstrated by mapping a quantum state from three entangled optical modes to atomic ensembles. The improvement of the degree of atom entanglement is crucial for further application in quantum information [37].

High-efficiency storage and release of the quantum state of optical modes in quantum nodes, as well as the establishment of high-quality entanglement among multiple remote quantum nodes, are required in high-fidelity quantum communication [33,34] and quantum computation [35]. In particular, in the quantum state mapping approach to the construction of quantum-node entanglement, the entanglement is sensitive to the squeezing of input optical modes and the memory efficiency of quantum nodes [19,27,37]. Therefore, it is essential to explore high-efficiency quantum memory. The experimental realization of DV high-efficiency quantum interface has been successfully demonstrated by harnessing the optical cavity to enhance the interaction between light and atomic spin waves [38–40]. However, CV quantum memory with high efficiency for entangled optical modes still remains challenging, which enables high-fidelity quantum information processing and high-quality entanglement among multiple quantum memories.

In this paper, by combining the generation technology of CV multipartite entanglement of optical modes using optical parametric amplifiers (OPAs) and the idea of quantum state transfer from entangled optical modes to atomic ensembles via cavity-enhanced quantum memory, we propose a deterministic and scalable generation system of Greenberger-Horne-Zeilinger-like (GHZ-like) entanglement among multiple spatially separated atomic ensembles. Quantum memory has the capability of capturing, storing, and releasing a fast-flying quantum state with a stationary matter system on demand. Electromagnetically induced transparency (EIT) dynamics is one of the well-known approaches to quantum memory for a nonclassical state of light, because the low noise is included in the quantum memory process [41–43]. However, the memory efficiency is unavoidably imperfect. Thus we transfer the above-mentioned DV cavity-enhanced quantum interface scheme to CV quantum memory, together with the intracavity EIT technique [44,45]. The CV high-efficiency quantum memory without any extra

*zhyan@sxu.edu.cn

noises can be realized based on cavity-enhanced light-atom interaction. Afterward, cavity-enhanced quantum memory for multiple off-line prepared, entangled optical modes can be applied in establishing quantum entanglement among multiple atomic ensembles. Within the storage lifetime the stored atom entanglement can be transferred into multiple released optical modes at any desired time for verifying atom entanglement and conveying quantum information across the quantum network. By applying the inseparability criterion for Gaussian states, the dependences of multipartite entanglement among atomic ensembles and released optical modes from atomic ensembles on systematic parameters are theoretically investigated and the exactly calculated results demonstrate that the quantum correlation can be obviously improved with the help of cavity-enhanced quantum memory. The optimal experimental parameters are obtained, which can provide a direct reference for experiment implementation. Our scheme makes it possible to realize the CV high-efficiency quantum memory and to produce the high-quality deterministic entanglement among multiple quantum memory nodes.

The paper is organized as follows. The CV cavity-enhanced quantum memory and its corresponding mathematic analysis based on quantum Langevin equations are investigated in Sec. II. In Sec. III we study the performance of entanglement among multiple space-separated atomic ensembles. The multiple entangled optical modes are first prepared by means of coupling squeezed states of optical modes on a beam-splitter network. The CV multipartite atom entanglement is then generated by quantum state mapping from multiple entangled optical modes to atomic ensembles inside ring cavities. Finally, the entanglement among multiple atomic ensembles can be verified based on the released optical modes from atomic ensembles. A brief summary is provided in Sec. IV.

II. CONTINUOUS-VARIABLE CAVITY-ENHANCED QUANTUM MEMORY

In quantum optics, the optical field is represented by the annihilation operator $\hat{a}$ and the amplitude and phase quadratures $\hat{X}_L$ and $\hat{Y}_L$ of light correspond to the real and imaginary parts of the annihilation operator $\hat{a}$, as $\hat{X}_L = (\hat{a} + \hat{a}^\dagger)/\sqrt{2}$ and $\hat{Y}_L = (\hat{a} - \hat{a}^\dagger)/\sqrt{2}i$, with the canonical commutation relation $[\hat{X}_L, \hat{Y}_L] = i$. Meanwhile, the collective atomic spin wave is described by the Stokes operator $\hat{S} = \sum_i |g\rangle\langle m|$ and the amplitude and phase quadratures $\hat{X}_A$ and $\hat{Y}_A$ of the atom are associated with the y and z components of $\hat{S}_y$ and $\hat{S}_z$ of the Stokes operator $\hat{S}$ on the Bloch sphere, that is, $\hat{X}_A = (\hat{S} + \hat{S}^\dagger)/\sqrt{2} = \hat{S}_y/\sqrt{\langle \hat{S}_x \rangle}$ and $\hat{Y}_A = (\hat{S} - \hat{S}^\dagger)/\sqrt{2}i = \hat{S}_z/\sqrt{\langle \hat{S}_x \rangle}$, which obey the canonical commutation relation $[\hat{X}_A, \hat{Y}_A] = i$ [30,31].

The dark-state polariton theory demonstrates that the quantum state can be ideally transferred between light and collective atomic spin waves in the EIT process [46–49]. Our work focuses on the field with a single transverse mode matched to the memory device. For an input signal field to be stored, a complete mode expansion into the longitudinal modes of the input optical field is $\hat{A}(t)^{\text{in}} = u(t)_0^{\text{in}} \hat{a}_0^{\text{in}}$, where $\hat{a}_0^{\text{in}}$ is an optical mode operator and $u(t)_0^{\text{in}}$ is a temporal mode function of the input optical field, which determines the optical pulse shape. The input pulse shape is dynamically shaped in time to provide optimum

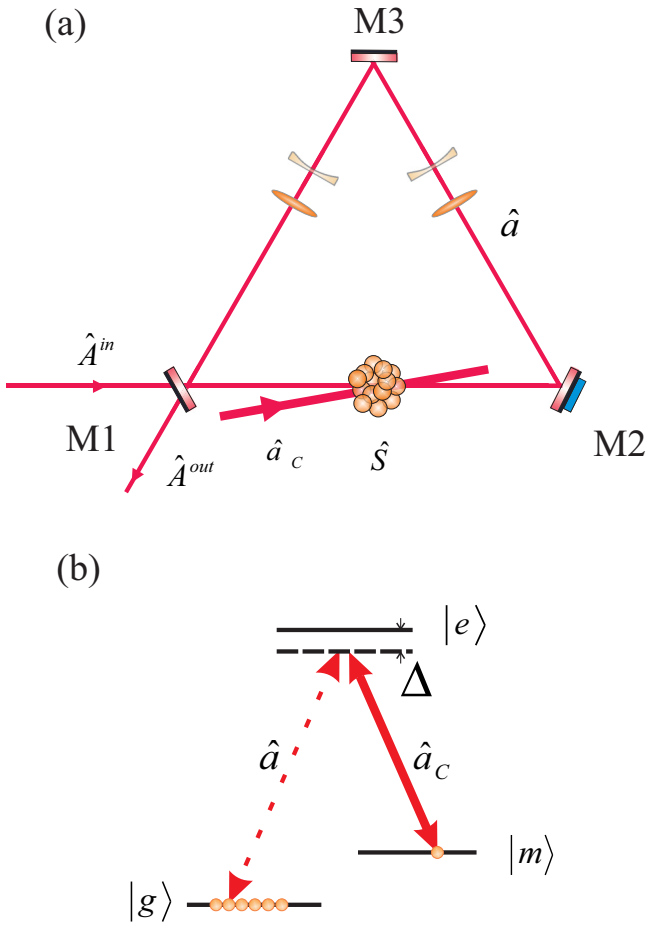

FIG. 1. (a) Schematic of the CV cavity-enhanced quantum memory system. (b) Atomic energy level for quantum memory. Atoms with a ground state $|g\rangle$, a metastable state $|m\rangle$, and an excited state $|e\rangle$ are shown.

coupling and mapping efficiency; the temporal mode function in our system is described by $u(t)_0^{\text{in}} = ce^{(\gamma_1+\gamma_2+\gamma_0)t/2} sh(mt)/m$, where $c = -i\sqrt{2[(\gamma_1+\gamma_2)\gamma_0 + g^2](\gamma_1+\gamma_2+\gamma_0)}$ and $m = \sqrt{[(\gamma_1+\gamma_2-\gamma_0)/2]^2 - g^2}$. For the output optical field $\hat{A}(t)^{\text{out}} = \int u(t)_0^{\text{out}} \hat{a}(t)^{\text{out}} dt$ and the appropriate selection of mode matched filters, the output optical mode can be obtained with high efficiency and the output temporal mode function is $u(t)_0^{\text{out}} = u(T_0 - t)_0^{\text{in}}$ [50].

The schematic of the cavity-enhanced quantum memory system composed of an atomic ensemble and optical cavity with a ring configuration is shown in Fig. 1(a). The atom with a λ-type three-energy-level structure of a ground state $|g\rangle$, a metastable state $|m\rangle$, and an excited state $|e\rangle$ is employed in EIT dynamics, which is presented in Fig. 1(b). The signal field is resonant with the transition between a ground state $|g\rangle$ and an excited state $|e\rangle$, while the control field is at a different wavelength resonant with the transition between a metastable state $|m\rangle$ and an excited state $|e\rangle$. In our system, the control field is much stronger than the signal field and thus is treated as a classical field. When the collective atomic spin wave $\hat{S}(t)$ interacts with the signal field $\hat{a}(t)$ via EIT dynamics, the quantum state of the signal light and the atomic ensemble can be converted to each other. In a rotating frame resonant with

the input carrier frequency of the quantum signal, the effective Hamiltonian $\hat{H}_{\rm EIT}$ of the light-atom interaction is similar to a beam-splitter interaction, as [50,51]

$$\hat{H}_{\rm EIT} = \hbar g \hat{a}^{\dagger}\hat{S} + \hbar g \hat{S}^{\dagger}\hat{a}, \tag{1}$$

where g is the effective light-atom interaction constant ($g = \sqrt{N_a}\mu\Omega/\Delta$). Here N_a is the number of atoms, μ is the light-atom coupling coefficient, Ω is the Rabi frequency of the control field, and Δ is the detuning of the light and atom coupling [33,51]. The three stages of the quantum memory process are writing, storage, and reading. The time scale of adiabatically switching on and off is about 40 ns. The user-controlled time in our system is taken as 1 μs and the storage lifetime in the hot atomic ensemble is about 10 μs [37], which can be extended to the time scale of milliseconds with a paraffin-coated cell [30]. If a cold atomic ensemble is confined in an optical lattice, the storage lifetime can reach a time scale of seconds [39]. Therefore, the steplike function used as an approximation of the switching on and off process in EIT dynamics in Eq. (1) is shown as follows: $\hat{H}(t) = \hat{H}_{\rm EIT}$, $-\infty < t < 0$; $\hat{H}(t) = 0$, $0 < t < T_0$; and $\hat{H}(t) = \hat{H}_{\rm EIT}$, $T_0 < t < \infty$. The light-atom interaction is modulated with a control field. (i) In the writing process ($-\infty < t < 0$), first, both the weak signal and strong control fields interact with an atomic medium, so the atomic medium becomes transparent and the group velocity for the signal field is greatly reduced. Then the writing process occurs up to a time $t = 0$. As the whole signal pulse is totally compressed in the atomic medium, the control field is adiabatically switched off, so the dark-state polariton is completely stopped in the atomic medium and the quantum state of light is transferred into that of the atomic medium. (ii) In the storage process ($0 < t < T_0$), within the storage lifetime, the atom can preserve the quantum state of light. (iii) In the reading process ($T_0 < t < \infty$), at the user-controlled time $t = T_0$, the reading process and the quantum state can be transferred from the atomic ensemble to the released optical mode by adiabatically switching on the control field again. Therefore, at the moment of $t = 0$, the quantum state is transferred from the light to the atom; at time $t = T_0$, the inverse quantum state transfer happens.

The performance of quantum memory can be improved by means of enhancing the interaction between the light and atoms via an optical cavity without introducing any extra noise. The optical cavity with a ring configuration consists of three flat mirrors and four lenses, as shown in Fig. 1(a). The input signal mode $\hat{A}(t)^{\rm in}$, which is to be stored, can be coupled into the cavity mode $\hat{a}$ through the input-output mirror with the coupling rate to the cavity of the input and output fields γ_1 ($\gamma_1 = T/2\tau$, where T is the transmissivity of the input-output mirror and τ is the round-trip time of the optical mode inside the optical cavity) and also the input-output mirror couples the output optical mode $\hat{A}(t)^{\rm out}$ out of the cavity. The other two cavity mirrors are highly reflective for the signal optical mode and one of them is mounted on the piezoelectric transducer for scanning or locking the cavity length, so the signal field resonates with the cavity mode. The four lenses with antireflection coating are used to enlarge the beam size of the cavity mode $\hat{a}$ so that the interaction area between the light and atoms can be increased and the mapping efficiency can be improved. The intracavity loss L is unavoidable in real experiments as a result of imperfect optical components and the corresponding decay rate of the intracavity loss is γ_2 ($\gamma_2 = L/2\tau$), which introduces the vacuum noise $\hat{A}(t)_{\upsilon}^{\rm in}$. The spin wave decoherence rate is γ_0, which couples the noise of the atomic medium $\hat{S}(t)_{\upsilon}$ into the cavity mode $\hat{a}$. The EIT interaction is enhanced by the feedback of the optical cavity. The quantum Langevin equations describing the evolution of observable operators for the cavity mode $\hat{a}(t)$ and collective atomic spin wave $\hat{S}(t)$ inside an optical cavity are

$$\begin{aligned}\frac{d\hat{a}(t)}{dt} &= -(\gamma_1+\gamma_2)\hat{a}(t) - ig(t)\hat{S}(t) \\ &\quad +\sqrt{2\gamma_1}\hat{A}(t)^{\rm in} + \sqrt{2\gamma_2}\hat{A}(t)_{\upsilon}^{\rm in}, \\ \frac{d\hat{S}(t)}{dt} &= -\gamma_0\hat{S}(t) - ig(t)\hat{a}(t) + \sqrt{2\gamma_0}\hat{S}(t)_{\upsilon}. \end{aligned} \tag{2}$$

The quantum memory process is usually considered as a beam-splitter interaction and the vacuum noise is added to the input state as a result of limited memory efficiency [37,50,51]. Due to the imperfect experiment, the intracavity loss is also considered in our theory. When the control field playing the role of writing process is on, the input signal mode is compressed in the atomic ensemble. At the moment of adiabatically turning off the control optical field, the quantum state is transferred from the input signal mode $\hat{a}_0^{\rm in}$ to the collective atomic spin wave $\hat{S}(0)$. By solving the quantum Langevin equations of the beam-splitter model with the proper input temporal mode function, the expression of the atomic spin wave $\hat{S}(0)$ inside the cavity can be obtained. When the control field propagates through the EIT medium, the Raman scattering process occurs and generates an excess noise, because the strong control field interacts with the atomic medium [42,52]. This excess noise is treated as an additional term in the result, which is similar to the treatment of noise in the cavity optomechanical system [53]. Luckily, the excess noise can be reduced by optimizing the memory system, so EIT-based memory is suitable for the nonclassical state of light. In the experiment, the excess noise is elevated by about 0.1 dB with respect to the vacuum due to the Raman scattering of the control field [42]. The Raman excess noises in the writing and reading processes are supposed to be equal: $V_W = V_R = V$. Thus the stored atomic spin wave is [50]

$$\begin{aligned}\hat{S}(0) &= \frac{\sqrt{\gamma_1}g}{\sqrt{(g^2+\gamma_0\gamma_1+\gamma_0\gamma_2)(\gamma_0+\gamma_1+\gamma_2)}}\hat{a}_0^{\rm in} \\ &\quad +\frac{\sqrt{g^2(\gamma_0+\gamma_2)+\gamma_0(\gamma_1+\gamma_2)(\gamma_0+\gamma_1+\gamma_2)}}{\sqrt{(g^2+\gamma_0\gamma_1+\gamma_0\gamma_2)(\gamma_0+\gamma_1+\gamma_2)}}\hat{a}_1^{r} + V_W, \end{aligned} \tag{3}$$

which agrees with the result of the cavity optomechanics system [53]. Here $\hat{a}_1^r$ is loss reservoir associated with the noise operator and V_W is the excess noise in the writing process. The corresponding writing mapping efficiency $\eta(0)_W$ from the input signal mode $\hat{a}_0^{\rm in}$ to the collective atomic spin wave $\hat{S}(0)$ is given by

$$\eta(0)_W = \frac{\gamma_1 g^2}{(g^2+\gamma_0\gamma_1+\gamma_0\gamma_2)(\gamma_0+\gamma_1+\gamma_2)}. \tag{4}$$

After the writing process, the collective atomic spin wave $\hat{S}(0)$ will evolve to $\hat{S}(T_0)$ at the storage duration of T_0 as a result of spin wave decoherence. By turning on the control fields again, the reading process happens and the stored quantum state in the atomic ensemble can be transferred back to that of the released optical mode. According to the quantum Langevin equations and the boundary condition on the input-output coupling mirror $\hat{a}(t)^{\text{out}} = \sqrt{2\gamma_1}\hat{a}(t) - \hat{A}(t)_\upsilon$, where $\hat{A}(t)_\upsilon$ is vacuum noise from the coupling mirror, the expression of the released optical field $\hat{A}(T_0)^{\text{out}}$ from the atomic ensemble at the storage duration of T_0 is [50]

$$\hat{A}(T_0)^{\text{out}} = \frac{\gamma_1 g^2 e^{-\gamma_0 T_0} - \gamma_1\gamma_0^2 e^{-(\gamma_1+\gamma_2)T_0}}{(g^2+\gamma_0\gamma_1+\gamma_0\gamma_2)(\gamma_0+\gamma_1+\gamma_2)}\hat{a}_0^{\text{in}} + \frac{\sqrt{(\gamma_0+\gamma_1+\gamma_2)^2(g^2+\gamma_0\gamma_1+\gamma_0\gamma_2)^2 - \left(\gamma_1 g^2 e^{-\gamma_0 T_0} - \gamma_1\gamma_0^2 e^{-(\gamma_1+\gamma_2)T_0}\right)^2}}{(g^2+\gamma_0\gamma_1+\gamma_0\gamma_2)(\gamma_0+\gamma_1+\gamma_2)}\hat{a}_2^r + V_R, \tag{5}$$

where $\hat{a}_2^r$ is both the reservoir operator arising from the noise and the excess noise in the reading process caused by Raman scattering of the control field. The total mapping efficiency $\eta(T_0)_T$ from the input optical mode $\hat{a}_0^{\text{in}}$ to the released optical mode $\hat{a}(T_0)^{\text{out}}$, which is a product of the writing efficiency $\eta(T_0)_W$ and reading efficiency $\eta(T_0)_R$ [$\eta(T_0)_T = \eta(T_0)_W\eta(T_0)_R$], is given by

$$\eta(T_0)_T = \frac{\left(\gamma_1 g^2 e^{-\gamma_0 T_0} - \gamma_1\gamma_0^2 e^{-(\gamma_1+\gamma_2)T_0}\right)^2}{(g^2+\gamma_0\gamma_1+\gamma_0\gamma_2)^2(\gamma_0+\gamma_1+\gamma_2)^2}. \tag{6}$$

To explore the advantage of CV cavity-enhanced quantum memory, Figs. 2(a) and 2(b) show that the writing mapping efficiency $\eta(0)_W$ and total mapping efficiency $\eta(T_0)_T$ depend on the the transmissivity T of the input-output mirror and intracavity loss L. All the other parameters are experimentally

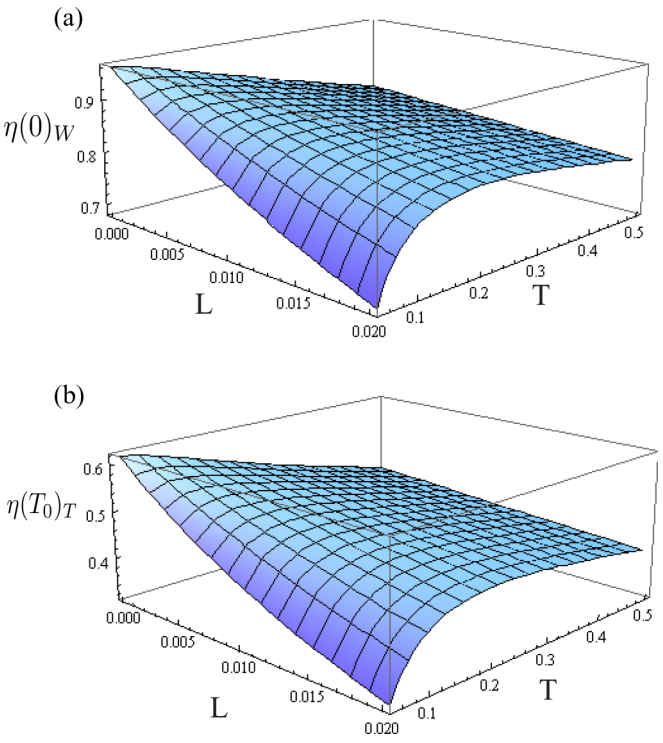

FIG. 2. Performance of CV memory efficiency as a function of the transmissivity T of the input-output mirror and intracavity loss L for (a) writing mapping efficiency $\eta(0)_W$ and (b) total mapping efficiency $\eta(T_0)_T$ at a storage time of 1 μs.

reachable: The effective light-atom coupling constant g is 10 MHz, the spin wave decoherence rate γ_0 caused by atomic decoherence is 0.2 MHz, the round-trip time τ of light in the cavity is 2.35 ns, the Raman excess noise is evaluated by 0.05 dB with respect to the vacuum, and the storage time T_0 is 1 μs. We find that the features of $\eta(0)_W$ and $\eta(T_0)_T$ can be obviously improved when the transmissivity T of the input-output mirror is under the appropriate condition. In addition, $\eta(0)_W$ and $\eta(T_0)_T$ are also sensitive to the intracavity loss L . When the intracavity loss L is smaller, the better performance of cavity-enhanced quantum memory can be realized. It can be seen that $\eta(0)_W$ and $\eta(T_0)_T$ can reach the maximum values $\eta(0)_W = 0.87$ and $\eta(T_0)_T = 0.51$ when the proper transmissivity of the input-output mirror $T = 0.15$ with the intracavity loss $L = 0.01$ is taken into account.

In quantum memory, the fidelity $F = \text{Tr}[(\hat{\rho}_1^{1/2}\hat{\rho}_2\hat{\rho}_1^{1/2})^{1/2}]^2$ describes the overlap of input states $\hat{\rho}_1$ with the states $\hat{\rho}_2$ stored in or released from the memory node and quantifies the level of memory performance and accuracy. Nha and Carmichael [54] and Scutaru [55] have demonstrated the calculations of fidelity for the Gaussian state. The memory fidelity for a set of predetermined Gaussian states $\hat{\rho}_1$ and determined Gaussian states $\hat{\rho}_2$ with covariance matrices A_j and mean amplitudes α_j ($j = 1,2$) is calculated as $F = \{2\exp[-\epsilon^T(A_1+A_2)^{-1}\epsilon]\}/(\sqrt{\Delta+\sigma}-\sqrt{\sigma})$, where $\Delta = \det(A_1+A_2)$, $\sigma = \det(A_1-1)\det(A_2-1)$, and $\epsilon = \alpha_2-\alpha_1$. The calculation of fidelity depends on the covariance matrices of the predetermined Gaussian states and determined Gaussian states [54–56]. The time-dependent operators of the atomic spin wave and released optical mode in quantum memory, which are shown in Eqs. (3) and (5), can be attained by solving the quantum Langevin equations in the Heisenberg picture. In quantum mechanics, the covariance matrix contains the information of the quantum system and can be derived from either time-dependent operators in the Heisenberg picture or the time-dependent state (density operator) in the Schrödinger picture. Based on the time-dependent operators, the covariance matrices ($j = 1,2$) for the input (output) mode are given by $A_j = 4\begin{bmatrix}\langle\Delta^2\hat{X}(t)\rangle_j & 0\\ 0 & \langle\Delta^2\hat{Y}(t)\rangle_j\end{bmatrix}$. Since in the fidelity formula the vacuum noise is normalized to 1, a coefficient 4 appears in the expressions of covariance matrices [56]. Thus quantum memory fidelities can be obtained from time-dependent operators [the above solutions (3) and (5)] by means of covariance matrices. Figures 3(a) and 3(b) show the dependence of the CV writing mapping fidelity $F(0)_W$ and total mapping fidelity

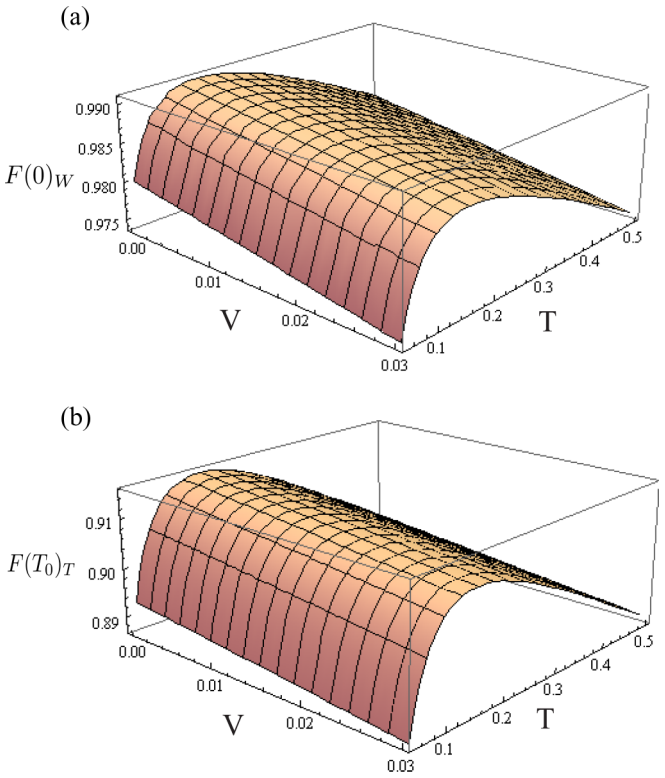

FIG. 3. Dependence of CV memory fidelity on the transmissivity T of the input-output mirror and Raman excess noise V for (a) writing mapping fidelity $F(0)_W$ and (b) total mapping fidelity $F(T_0)_T$ at a storage time of 1 μs.

$F(T_0)_T$ on the transmissivity T of the input-output mirror and Raman excess noise V in the memory process with the 5 dB input squeezed state of light resonant with the atomic absorption line [57]. It can be seen that the performance of $F(0)_W$ and $F(T_0)_T$ can be increased when the transmissivity T of the input-output mirror is under the appropriate condition. The Raman excess noise V will decrease $F(0)_W$ and $F(T_0)_T$. The maximum values of $F(0)_W$ and $F(T_0)_T$ can be obtained as $F(0)_W = 0.99$ and $F(T_0)_T = 0.86$, with the optimal transmissivity and a Raman excess noise V of 0.012. Therefore, the optical cavity can enhance the interaction between the light and atoms so that the writing mapping efficiency $\eta(0)_W$ [fidelity $F(0)_W$] and total mapping efficiency $\eta(T_0)_T$ [fidelity $F(T_0)_T$] can be greatly increased compared with the previous implementation without an optical cavity [42,43].

III. UNCONDITIONAL ENTANGLEMENT AMONG MULTIPLE SPATIALLY SEPARATED ATOMIC ENSEMBLES

Quantum state mapping is one of the effective approaches to establish macroscopic object entanglement and the mapping efficiency is important for the entanglement quality [19,27,37]. In our proposal, the unconditional GHZ-like entangled state among multiple distant atomic ensembles is generated by mapping the multipartite entangled state from optical modes to atomic ensembles via CV cavity-enhanced quantum memory. For a generation system of N entangled atomic ensembles, the nonclassical light source involves N OPAs and $N-1$ beam

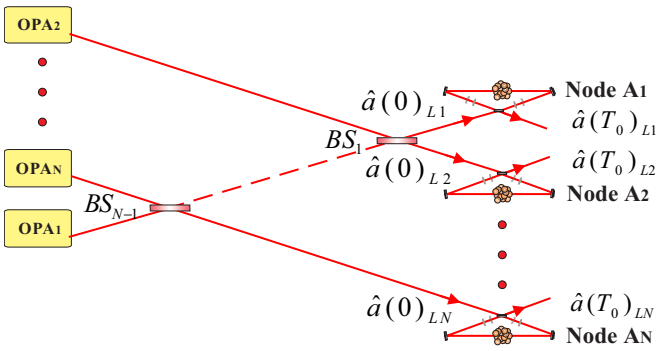

FIG. 4. Generation and verification schematic of deterministic entanglement among N spatially separated atomic ensembles.

splitters; in addition, N cavity-enhanced quantum memories are employed as quantum nodes. The off-line prepared N entangled optical modes are produced by coupling N squeezed states from OPAs on $N-1$ beam splitters. Quantum entanglement among N atomic ensembles is established by means of efficient quantum state mapping from the resulting N entangled optical modes to N atomic ensembles under the writing interaction in cavity-enhanced EIT dynamics. Within the storage lifetime, the multipartite entanglement can be preserved in atomic ensembles. At a user-controlled time, the entanglement can be transferred from atomic ensembles to released optical modes for entanglement verification. The generation and verification schematic of deterministic entanglement among N spatially separated atomic ensembles is displayed in Fig. 4, where the quantum node A_i ($i = 1,2,\ldots,N$) stands for CV cavity-enhanced quantum memory. There are N OPAs and $N-1$ beam splitters involved in the system. For quantum entanglement among three quantum nodes, three OPAs and two beam splitters are required.

In quantum technology, the OPA is a well-understood device for generating nonclassical optical fields. Further, a single OPA can produce multipartite entangled optical modes with different frequencies [58,59]; multiple spatially separated entangled optical modes can be obtained based on linear coupling squeezed states of light on beam splitters [60]. The down-converted optical fields $\hat{a}_{Si}$ are generated under the nonlinear interaction with the pump optical fields, which are much stronger than signal fields and treated as classical fields. The Hamiltonian $\hat{H}_{\rm sq}$ of the squeezing interaction is of parametric gain type,

$$\hat{H}_{\rm sq} = i\hbar\kappa\hat{a}_{Si}^{\dagger 2} - i\hbar\kappa^*\hat{a}_{Si}^2, \tag{7}$$

where the nonlinear coupling strength $\kappa = \beta\chi e^{i\theta}$ is proportional to the pump parameter β (with χ the nonlinear susceptibility of the nonlinear medium), and is the relative phase between the signal field and pump field. The OPA_1 is operated at the condition of parametric amplification ($\theta = 0$) to generate the quadrature phase squeezed state $\hat{a}_{s1}$, while the remaining optical modes of the OPA_j ($j = 2,3,\ldots,N$) are running in the case of parametric deamplification ($\theta = \pi$) to produce the quadrature amplitude squeezed state $\hat{a}_{sj}$ [61,62]. According to the Heisenberg motion equations, describing the evolution of optical fields in the nonlinear process, the N output

optical fields of the OPAs are obtained as $\hat{a}_{S1} = chr1\hat{a}_{S1}^{\rm in} + shr1\hat{a}_{S1}^{\rm in\dagger}$ and $\hat{a}_{Sj} = chr2\hat{a}_{Sj}^{\rm in} - shr2\hat{a}_{Sj}^{\rm in\dagger}$, where $\hat{a}_{Si}^{\rm in}$ is the input coherent state for the OPA$_i$. The squeezing parameters ri for all the OPAs are assumed to be identical for simplicity and are proportional to the nonlinear coupling strength κ and interaction time τ' between the light and nonlinear crystal, $ri = r = \kappa\tau'$. The squeezing parameter $r = 0.6$ is taken into account, which corresponds to the ∼5 dB squeezed state of light [57].

The phase-free beam-splitter operation on a pair of modes p and q, $\hat{B}_{pq}(\theta)$, is $\hat{a}_p \to \hat{a}_p\cos\theta + \hat{a}_q\sin\theta$ and $\hat{a}_q \to \hat{a}_p\sin\theta - \hat{a}_q\cos\theta$. By applying the beam-splitter network $\hat{N}_{1,\ldots,N} = \hat{B}_{N-1N}(\pi/4)\hat{B}_{N-2N-1}(\cos^{-1}1/\sqrt{3})\cdots\hat{B}_{12}(\cos^{-1}1/\sqrt{N})$, the N-party entangled state of optical modes $\hat{a}_{Li}$ is obtained via superimposing a quadrature phase squeezed state $\hat{a}_{s1}$ and $N-1$ quadrature amplitude squeezed states $\hat{a}_{sj}$, and the output space-separated optical modes can be chopped into optical pulses and distributed to multiple distant quantum nodes [61,62].

The performance of quantum entanglement among the atomic spin waves or optical modes of the N-party Gaussian entangled state can be verified by the inseparability criteria [63]

$$\langle\delta^2(\hat{X}_l - \hat{X}_m)\rangle + \left\langle\delta^2\left(\hat{Y}_l + \hat{Y}_m + g^{(N)}\sum_{n\neq l,m}^{N}\hat{Y}_n\right)\right\rangle < 1. \quad (8)$$

Here $l,m,n = 1,\ldots\ldots,N$ and $g^{(N)}$ is the optimal gain factor to minimize the correlation variances on the left-hand side of Eq. (8). The value 1 on the right-hand side of Eq. (8) is the corresponding boundary for the inseparable state; the vacuum noise is normalized to 1/4 in the inseparability criteria. If $N-1$ inequalities are simultaneously satisfied, N atomic spin waves or optical modes are entangled. The smaller the value of the combination of correlation variances on the left-hand side of Eq. (8), the better the quality of multipartite entanglement. The time-dependent operators of atomic spin waves and released optical modes can be obtained from the solutions of the quantum Langevin equations (3) and (5). By substituting the expression of each optical mode of the N-party entangled optical fields for $\hat{a}_0^{\rm in}$ in Eqs. (3) and (5), the operators of the atomic spin wave and released optical modes can be derived. According to the definition of quadrature components, the value of the combination of correlation variances on the left-hand side of the inseparability criterion can be obtained to check the quantum entanglement among N atomic ensembles in the cavities and released optical modes [37,61–63].

The entanglement among optical modes can be characterized according to the multipartite inseparability criterion for the Gaussian state. The combinations of correlation variances for optical modes in the inseparability criterion are equal $[I(0)_{L1} = \cdots = I(0)_{LN} = I(0)_L]$,

$$\begin{aligned} I(0)_L &= \langle\delta^2(\hat{X}_{Ll} - \hat{X}_{Lm})\rangle \\ &\quad + \left\langle\delta^2\left(\hat{Y}_{Ll} + \hat{Y}_{Lm} + g_L^{(N)}\sum_{n\neq l,m}^{N}\hat{Y}_{Ln}\right)\right\rangle \\ &= \frac{1}{2}e^{-2r2} + \frac{\left[2+(N-2)g_L^{(N)}\right]^2}{4N}e^{-2r1} \\ &\quad + \frac{(N-2)\left(g_L^{(N)}-1\right)^2}{2N}e^{2r2}. \end{aligned} \quad (9)$$

The optimal gain factor $g_L^{(N)}$ is used to minimize the value of the combination of correlation variances on the left-hand side of Eq. (9) for optical modes. The performance of entanglement can be improved by choosing the proper value of the optimal gain factor. If $I(0)_L < 1$, the output modes from beam-splitter network form a GHZ-like state [61–63].

The quantum correlation among N atomic ensembles is established by mapping the quantum state from the input entangled optical modes to the atomic ensembles inside the ring cavities. The output optical modes $\hat{a}_{Li}$ from the beam-splitter network are used as input signal optical fields $\hat{A}(t)_i^{\rm in}$ of cavity-enhanced quantum memory and coupled into the cavity modes $\hat{a}_i$ through the input-output mirrors so that the quantum state can be efficiently transferred from optical modes into atomic ensembles. The multipartite inseparability criterion can be applied in verifying entanglement among multiple atomic ensembles. All the OPAs and atomic cells are supposed to be in the same condition, so the combinations of correlation variances for atomic ensembles are identical, i.e., $I(0)_{A1} = \cdots = I(0)_{AN} = I(0)_A$. The combination of correlation variances for N atomic ensembles in the inseparability criterion is obtained as

$$\begin{aligned} I(0)_A &= \langle\delta^2(\hat{X}_{Al} - \hat{X}_{Am})\rangle \\ &\quad + \left\langle\delta^2\left(\hat{Y}_{Al} + \hat{Y}_{Am} + g_A^{(N)}\sum_{n\neq l,m}^{N}\hat{Y}_{An}\right)\right\rangle \\ &= \frac{1}{2}\eta(0)_W e^{-2r2} + \frac{\left[2+(N-2)g_A^{(N)}\right]^2}{4N}\eta(0)_W e^{-2r1} \\ &\quad + \frac{(N-2)\left(g_A^{(N)}-1\right)^2}{2N}\eta(0)_W e^{2r2} + 1 - \eta(0)_W \\ &\quad + \frac{(N-2)(1-\eta(0)_W)}{4}g_A^{(N)2}, \end{aligned} \quad (10)$$

where $g_A^{(N)}$ is the optimal gain factor to optimize the value of the combination of correlation variances on the left-hand side of Eq. (10) for atomic spin waves. If $I(0)_A$ is less than 1, the GHZ-like atom entanglement exists [37].

Figure 5 demonstrates the dependence of the combination of correlation variances $I(0)_A$ for atomic ensembles on the transmissivity T of the input-output mirror with the intracavity loss $L = 0.01$, while the other parameters are kept the same as those of above cavity-enhanced quantum memory condition. The traces labeled with $N = 3$, 9, 14, and 15 represent the combination of correlation variances for 3, 9, 14, and 15 parties, respectively. The trace of the corresponding quantum noise limit (QNL) is labeled. The smaller $I(0)_A$ is, the better the atom entanglement is. We can see that $I(0)_A$ almost reaches a minimum value of 0.49 for three atomic ensembles, when the value of the transmissivity T of the input-output mirror is 0.15. As long as $I(0)_A$ is less than 1, the GHZ-like entanglement among multiple atomic ensembles is proved. Therefore,

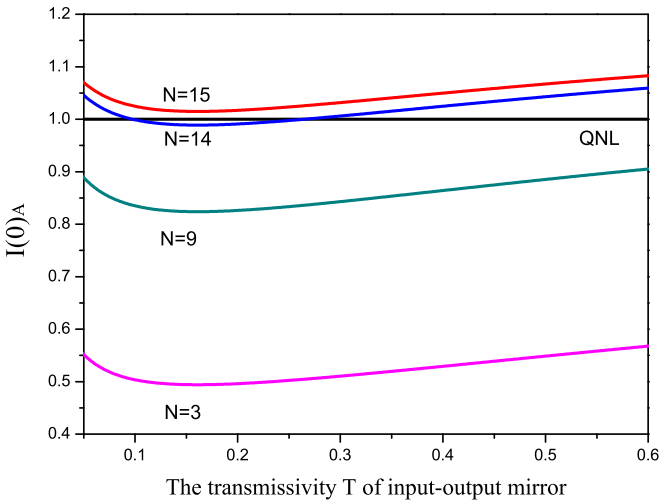

FIG. 5. Dependence of the combination of correlation variances for atomic ensembles of different numbers of parties $N = 3$, 9, 14, and 15 on the transmissivity T of input-output mirror.

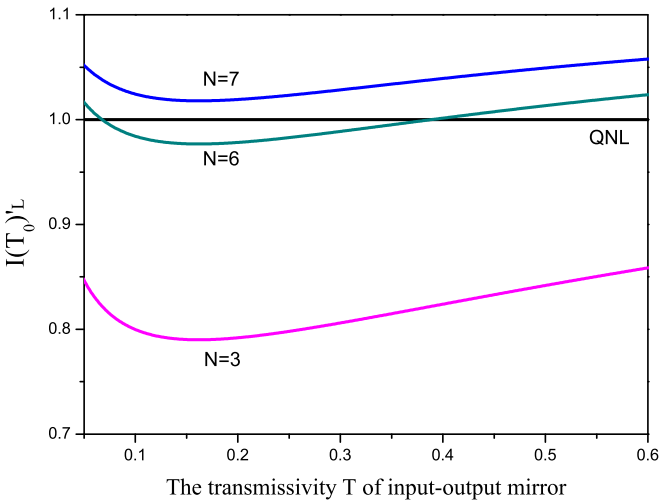

FIG. 7. Combination of correlation variances for the released optical modes of different numbers of parties $N = 3$, 6, and 7 vs the transmissivity T of the input-output mirror at a storage time of 1 μs.

entanglement among N ($N \leqslant 14$) atomic ensembles can be obtained.

The function of the combination of correlation variances $I(0)_A$ for atomic ensembles on the intracavity loss L is illustrated in Fig. 6, where the transmissivity T of the input-output mirror is 0.15. The traces labeled with $N = 3$, 9, and 14 stand for the combination of correlation variances for 3, 9, and 14 parties, respectively. The intracavity loss L influences the performance of atom entanglement. The atom entanglement will disappear with an increase of the intracavity loss L. The intracavity loss L can be reduced by improving the quality of optical components. For N ($N \leqslant 14$) atomic ensembles, atom entanglement exists when $L < 0.01$.

In order to verify the quantum entanglement among multiple atomic ensembles, the quantum state can be converted from atomic ensembles into the released optical modes in the reading process by turning on the control optical fields again. The performance of the combination of correlation variances $I(T_0)'_L$ $[I(T_0)'_L = \langle\delta^2(\hat{X}'_{Lm} - \hat{X}'_{Ln})\rangle + \langle\delta^2(\hat{Y}'_{Lm} + \hat{Y}'_{Ln} + g_L^{\prime(N)}\sum_{l\neq m,n}^{N}\hat{Y}'_{Ll})\rangle]$ for the released optical modes from atomic ensembles at a storage time of 1 μs with a Raman excess noise of 0.1 dB is studied in Fig. 7, where $g_L^{\prime(N)}$ is the optimal gain factor for the released optical mode from atomic ensembles. The traces labeled with $N = 3$, 6, and 7 are the combination of correlation variances for 3, 6, and 7 parties, respectively. The optimal experimental conditions for the released optical modes are similar to those for atom entanglement, as a result of the linear mapping relation in the quantum memory process. From Fig. 7 we can see that the combination of correlation variances $I(T_0)'_L$ of the released optical modes from atomic ensembles can reach 0.79 for tripartite atom entanglement. As shown in Fig. 4, quantum entanglement among N ($N \leqslant 14$) atomic ensembles exists, but it cannot be verified by means of the released optical modes. When $N \leqslant 6$ the released optical modes are in an entangled state, which demonstrates that quantum nodes have the capacity to preserve 6-party entanglement. Thus N-party ($N \leqslant 6$) atom entanglement can be generated based on the quantum mapping approach and confirmed by making use of the released optical modes.

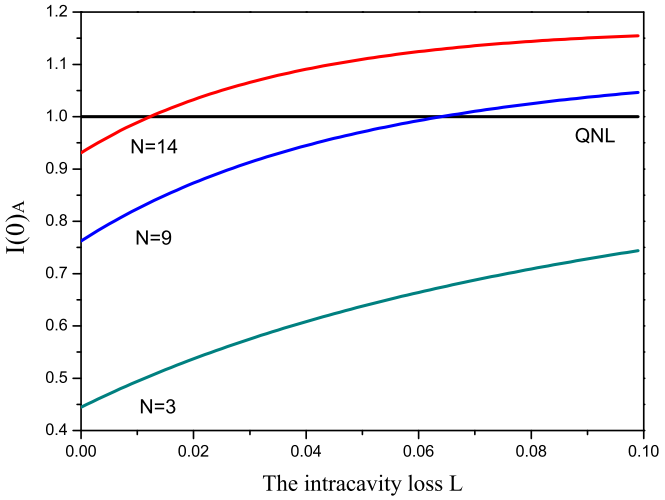

FIG. 6. Function of the combination of correlation variances for atomic ensembles of different numbers of parties $N = 3$, 9, and 14 on the intracavity loss L.

According to the theoretical analysis, an optimal value of the transmissivity T of the input-output mirror of 0.15 is taken into account when the intracavity loss L is 0.01, the squeezed degree of input optical beams is 5 dB, and the Raman excess noise is $V = 0.012$. The writing mapping efficiency (fidelity) can reach 0.87 (0.99) and the combination of correlation variances in the inseparability criterion for three atomic ensembles can be 0.49 under proper conditions.

IV. CONCLUSION

We have designed a deterministic and scalable entanglement generation scheme of multiple spatially separated atomic

ensembles based on CV cavity-enhanced quantum memory. The memory efficiency is improved without introducing any extra noise by means of cavity-enhanced interaction between light and an atomic ensemble. The CV cavity-enhanced quantum memory can be applied in high-fidelity quantum information processing [33–35], atom entanglement distillation [64], and the production of quantum entanglement among multiple atomic ensembles by mapping the quantum state from multiple entangled optical modes into atomic ensembles inside optical cavities, which can be verified by making use of the released optical modes from atomic ensembles. The obtained entanglement quality among atomic ensembles depends on the writing mapping efficiency $\eta(0)_w$ of the atomic ensemble and the initial squeezing parameter r of OPAs. The writing mapping efficiency $\eta(0)_w$ can be improved by placing the quantum memory inside an optical cavity. Recently, the squeezing degree of optical squeezed states was able to reach 15 dB [65]. Our protocol can be directly extended to quantum networks with other quantum nodes, such as single atoms, trapped ions, optomechanics, superconductors, solid-state systems, and other physical systems. Therefore, the generation of high-quality multipartite entanglement among multiple macroscopic objects is possible, which enables the implementation of the potential applications in the quantum information task, such as quantum state transfer across a quantum network and distributed quantum computation.

ACKNOWLEDGMENTS

This research was supported by the Key Project of the National Key R&D program of China (Grant No. 2016YFA0301402), the National Natural Science Foundation of China (Grants No. 61775127, No. 11474190, and No. 11654002), Fok Ying Tung Education Foundation, the Program for Sanjin Scholars of Shanxi Province, Shanxi Scholarship Council of China, and the fund for Shanxi "1331 Project" Key Subjects Construction.

[1] S. L. Braunstein and P. van Loock, Rev. Mod. Phys. **77**, 513 (2005).
[2] J.-W. Pan, Z.-B. Chen, C.-Y. Lu, H. Weinfurter, A. Zeilinger, and M. Żukowski, Rev. Mod. Phys. **84**, 777 (2012).
[3] H. J. Kimble, Nature (London) **453**, 1023 (2008).
[4] J. Simon, H. Tanji, S. Ghosh, and V. Vuletic, Nat. Phys. **3**, 765 (2007).
[5] A. M. Marino, R. C. Pooser, V. Boyer, and P. D. Lett, Nature (London) **457**, 859 (2009).
[6] M. Hosseini, B. M. Sparkes, G. Campbell, P. K. Lam, and B. C. Buchler, Nat. Commun. **2**, 174 (2011).
[7] V. Parigi, V. Ambrosio, C. Arnold, L. Marrucci, F. Sciarrino, and J. Laurat, Nat. Commun. **6**, 7706 (2015).
[8] Z. Yan and X. Jia, Quantum Sci. Technol. **2**, 024003 (2017).
[9] Y.-F. Pu, N. Jiang, W. Chang, H.-X. Yang, C. Li, and L.-M. Duan, Nat. Commun. **8**, 15359 (2017).
[10] G. Colangelo, F. M. Ciurana, L. C. Bianchet, R. J. Sewell, and M. W. Mitchell, Nature (London) **543**, 525 (2017).
[11] H. P. Specht, C. Nolleke, A. Reiserer, M. Uphoff, E. Figueroa, S. Ritter, and G. Rempe, Nature (London) **473**, 190 (2011).
[12] A. Facon, E. K. Dietsche, D. Grosso, S. Haroche, J. M. Raimond, M. Brune, and S. Gleyzes, Nature (London) **535**, 262 (2016).
[13] C. Langer, R. Ozeri, J. D. Jost, J. Chiaverini, B. DeMarco, A. Ben-Kish, R. B. Blakestad, J. Britton, D. B. Hume, W. M. Itano, D. Leibfried, R. Reichle, T. Rosenband, T. Schaetz, P. O. Schmidt, and D. J. Wineland, Phys. Rev. Lett. **95**, 060502 (2005).
[14] A. Stute, B. Casabone, P. Schindler, T. Monz, P. O. Schmidt, B. Brandstätter, T. E. Northup, and R. Blatt, Nature (London) **485**, 482 (2012).
[15] D. Hucul, I. V. Inlek, G. Vittorini, C. Crocker, S. Debnath, S. M. Clark, and C. Monroe, Nat. Phys. **11**, 37 (2014).
[16] V. Fiore, Y. Yang, M. C. Kuzyk, R. Barbour, L. Tian, and H. Wang, Phys. Rev. Lett. **107**, 133601 (2011).
[17] H. Lee, M.-G. Suh, T. Chen, J. Li, S. A. Diddams, and K. J. Vahala, Nat. Commun. **4**, 2468 (2013).
[18] R. Riedinger, S. Hong, R. A. Norte, J. A. Slater, J. Shang, A. G. Krause, V. Anant, M. Aspelmeyer, and S. Gröblacher, Nature (London) **530**, 313 (2016).
[19] S. Kiesewetter, R. Y. Teh, P. D. Drummond, and M. D. Reid, Phys. Rev. Lett. **119**, 023601 (2017).
[20] E. Flurin, N. Roch, J. D. Pillet, F. Mallet, and B. Huard, Phys. Rev. Lett. **114**, 090503 (2015).
[21] C. Clausen, I. Usmani, F. Bussieres, N. Sangouard, M. Afzelius, H. D. Riedmatten, and N. Gisin, Nature (London) **469**, 508 (2011).
[22] E. Saglamyurek, N. Sinclair, J. Jin, J. A. Slater, D. Oblak, F. Bussieres, M. George, R. Ricken, W. Sohler, and W. Tittel, Nature (London) **469**, 512 (2011).
[23] M. Zhong, M. P. Hedges, R. L. Ahlefeldt, J. G. Bartholomew, S. E. Beavan, S. M. Wittig, J. J. Longdell, and M. J. Sellars, Nature (London) **517**, 177 (2015).
[24] W. B. Gao, P. Fallahi, E. Togan, J. Miguel-Sanchez, and A. Imamoglu, Nature (London) **491**, 426 (2012).
[25] C. W. Chou, H. D. Riedmatten, D. Felinto, S. V. Polyakov, S. J. van Enk, and H. J. Kimble, Nature (London) **438**, 828 (2005).
[26] D. N. Matsukevich, T. Chaneliere, S. D. Jenkins, S. Y. Lan, T. A. B. Kennedy, and A. Kuzmich, Phys. Rev. Lett. **96**, 030405 (2006).
[27] K. S. Choi, H. Deng, J. Laurat, and H. J. Kimble, Nature (London) **452**, 67 (2008).
[28] Z.-S. Yuan, Y.-A. Chen, B. Zhao, S. Chen, J. Schmiedmayer, and J.-W. Pan, Nature (London) **454**, 1098 (2008).
[29] W. Zhang, D.-S. Ding, M.-X. Dong, S. Shi, K. Wang, S.-L. Liu, Y. Li, Z.-Y. Zhou, B.-S. Shi, and G.-C. Guo, Nat. Commun. **7**, 13514 (2016).
[30] B. Julsgaard, A. Kozhekin, and E. S. Polzik, Nature (London) **413**, 400 (2001).
[31] H. Krauter, C. A. Muschik, K. Jensen, W. Wasilewski, J. M. Petersen, J. I. Cirac, and E. S. Polzik, Phys. Rev. Lett. **107**, 080503 (2011).
[32] Y. Liu, Z. Yan, X. Jia, and C. Xie, Sci. Rep. **6**, 25715 (2016).
[33] L. M. Duan, M. D. Lukin, J. I. Cirac, and P. Zoller, Nature (London) **414**, 413 (2001).
[34] N. Sangouard, C. Simon, H. D. Riedmatten, and N. Gisin, Rev. Mod. Phys. **83**, 33 (2011).

[35] S. D. Barrett, P. P. Rohde, and T. M. Stace, New J. Phys. **12**, 093032 (2010).
[36] K. S. Choi, A. Goban, S. B. Papp, S. J. van Enk, and H. J. Kimble, Nature (London) **468**, 412 (2010).
[37] Z. Yan, L. Wu, X. Jia, Y. Liu, R. Deng, S. Li, H. Wang, C. Xie, and K. Peng, Nat. Commun. **8**, 718 (2017).
[38] X.-H. Bao, A. Reingruber, P. Dietrich, J. Rui, A. Duck, T. Strassel, L. Li, N.-L. Liu, B. Zhao, and J.-W. Pan, Nat. Phys. **8**, 517 (2012).
[39] S.-J. Yang, X.-J. Wang, X.-H. Bao, and J.-W. Pan, Nat. Photon. **10**, 381 (2016).
[40] D. J. Saunders, J. H. D. Munns, T. F. M. Champion, C. Qiu, K. T. Kaczmarek, E. Poem, P. M. Ledingham, I. A. Walmsley, and J. Nunn, Phys. Rev. Lett. **116**, 090501 (2016).
[41] J. Cviklinski, J. Ortalo, J. Laurat, A. Bramati, M. Pinard, and E. Giacobino, Phys. Rev. Lett. **101**, 133601 (2008).
[42] J. Appel, E. Figueroa, D. Korystov, M. Lobino, and A. I. Lvovsky, Phys. Rev. Lett. **100**, 093602 (2008).
[43] K. Honda, D. Akamatsu, M. Arikawa, Y. Yokoi, K. Akiba, S. Nagatsuka, T. Tanimura, A. Furusawa, and M. Kozuma, Phys. Rev. Lett. **100**, 093601 (2008).
[44] H. B. Wu, J. Gea-Banacloche, and M. Xiao, Phys. Rev. Lett. **100**, 173602 (2008).
[45] M. Albert, A. Dantan, and M. Drewsen, Nat. Photon. **5**, 633 (2011).
[46] M. Fleischhauer, A. Imamoglu, and J. P. Marangos, Rev. Mod. Phys. **77**, 633 (2005).
[47] M. Fleischhauer and M. D. Lukin, Phys. Rev. Lett. **84**, 5094 (2000).
[48] Y.-H. Chen, M.-J. Lee, I.-C. Wang, S. Du, Y.-F. Chen, Y.-C. Chen, and I. A. Yu, Phys. Rev. Lett. **110**, 083601 (2013).
[49] Z. Xu, Y. Wu, L. Tian, L. Chen, Z. Zhang, Z. Yan, S. Li, H. Wang, C. Xie, and K. Peng, Phys. Rev. Lett. **111**, 240503 (2013).
[50] Q. Y. He, M. D. Reid, E. Giacobino, J. Cviklinski, and P. D. Drummond, Phys. Rev. A **79**, 022310 (2009).
[51] Z. Y. Ou, Phys. Rev. A **78**, 023819 (2008).
[52] M. T. L. Hsu, G. Hétet, O. Glöckl, J. J. Longdell, B. C. Buchler, H.-A. Bachor, and P. K. Lam, Phys. Rev. Lett. **97**, 183601 (2006).
[53] J. Zhang, K. Peng, and S. L. Braunstein, Phys. Rev. A **68**, 013808 (2003).
[54] H. Nha and H. J. Carmichael, Phys. Rev. A **71**, 032336 (2005).
[55] H. Scutaru, J. Phys. A **31**, 3659 (1998).
[56] X. Su, S. Hao, X. Deng, L. Ma, M. Wang, X. Jia, C. Xie, and K. Peng, Nat. Commun. **4**, 2828 (2013).
[57] Y. Han, X. Wen, J. He, B. Yang, Y. Wang, and J. Wang, Opt. Exp. **24**, 2350 (2016).
[58] S. Yokoyama, R. Ukai, S. C. Armstrong, C. Sornphiphatphong, T. Kaji, S. Suzuki, J. I. Yoshikawa, H. Yonezawa, N. C. Menicucci, and A. Furusawa, Nat. Photon. **7**, 982 (2013).
[59] J. Roslund, R. M. de Araújo, S. Jiang, C. Fabre, and N. Treps, Nat. Photon. **8**, 109 (2014).
[60] X. Su, Y. Zhao, S. Hao, X. Jia, C. Xie, and K. Peng, Opt. Lett. **37**, 5178 (2012).
[61] T. Aoki, N. Takei, H. Yonezawa, K. Wakui, T. Hiraoka, A. Furusawa, and P. van Loock, Phys. Rev. Lett. **91**, 080404 (2003).
[62] L. Wu, Z. Yan, Y. Liu, R. Deng, and X. Jia, Appl. Phys. Lett. **108**, 161102 (2016).
[63] P. van Loock and A. Furusawa, Phys. Rev. A **67**, 052315 (2003).
[64] A. Datta, L. Zhang, J. Nunn, N. K. Langford, A. Feito, M. B. Plenio, and I. A. Walmsley, Phys. Rev. Lett. **108**, 060502 (2012).
[65] H. Vahlbruch, M. Mehmet, K. Danzmann, and R. Schnabel, Phys. Rev. Lett. **117**, 110801 (2016).